



## Correct structural index defined by base level estimates in Euler deconvolution

Felipe Ferreira de Melo (Observatório Nacional)\* and Valeria Cristina Ferreira Barbosa (Observatório Nacional)

Copyright 2017, SBGf - Sociedade Brasileira de Geofísica

This paper was prepared for presentation during the 15<sup>th</sup> International Congress of the Brazilian Geophysical Society held in Rio de Janeiro, Brazil, 31 July to 3 August, 2017.

Contents of this paper were reviewed by the Technical Committee of the 15<sup>th</sup> International Congress of the Brazilian Geophysical Society and do not necessarily represent any position of the SBGf, its officers or members. Electronic reproduction or storage of any part of this paper for commercial purposes without the written consent of the Brazilian Geophysical Society is prohibited.

### Abstract

The main goal of Euler deconvolution is to define the source nature and its depth position. Besides that, it estimates base level of the data and horizontal positions of the sources. To define the correct structural index most authors take advantage of the clustering in depth estimates. Some authors assume constant, linear or nonlinear base levels in their formulation, thus they estimate or eliminate this parameter from their analysis. With a tentative structural index, we take advantage of base level clustering when the correct structural index is used. We modeled three bodies with different structural indices and show that minimum variation of depth is sufficient to indicate the correct structural index when no interfering anomalies are present. In the presence of interfering anomalies, the minimum variation of base level estimates indicates the correct structural index. We simulated constant and nonlinear base levels in our tests. Application to a real data set shows that nonlinear base level is present possibly due to interfering anomalies. These results are valid independent of geomagnetic field incidence.

### Introduction

Reid et al. (1990), based on previous works of Euler homogeneous function (Hood, 1965; Thompson, 1982) proposed Euler deconvolution. This technique, usually, assumes a tentative structural index, related to the nature of the source, and estimates four parameters: base level, horizontal and vertical positions. Structural index can only be integer (Reid et al., 2014; Reid and Thurston, 2014), otherwise the anomaly decay with distance would change in a discontinuous way as the distance source to observer changes. Ravat (1996) clearly has shown this behavior with synthetic tests of a dipole and a thin circular disk (arbitrarily shaped source).

Thompson (1982) noticed the relation between the use of the correct structural index and a tight clustering in depth estimates. He used this behavior to define the correct structural index and others like Reid et al. (1990) followed this approach. Barbosa et al. (1999) proposed that the minimum correlation between base level estimates and magnetic anomaly gives the correct structural index, Melo et al. (2013) used this approach in 3D data.

Some authors assume constant (Thompson, 1982; Reid et al., 1990; Barbosa et al., 1999; Hsu, 2002), linear

(Gerovska and Araújo-Bravo, 2003; Stavrev, 1997) and nonlinear (Dewangan et al., 2007) base levels. With different mathematical approaches, these authors estimated the base level, used to identify the correct structural index or eliminated from their formulation.

We use tentative structural index and analyze depth and base level estimates in order to define the correct structural index. We noticed that for non-interfering anomalies the minimum standard deviation of depth estimates gives the correct structural index. For interfering anomalies this criterion fails; however, the minimum standard deviation of base level estimates gives the correct structural index. Dewangan et al. (2007) pointed that nonlinear base levels can be generated for sources close to each other, interfering anomalies. Therefore, we made tests simulating constant and nonlinear base levels in order to understand their behavior. As we shall see in real data application, base level can be nonlinear and possibly generated by sources close to each other.

### Euler deconvolution

Considering a discrete set of  $N$  observations of total-field anomaly, Euler deconvolution (Reid et al., 1990) can be written as a linear system of equations given by:

$$\hat{x}_o \frac{\partial h_i}{\partial x} + \hat{y}_o \frac{\partial h_i}{\partial y} + \hat{z}_o \frac{\partial h_i}{\partial z} + n\hat{b} = x_i \frac{\partial h_i}{\partial x} + y_i \frac{\partial h_i}{\partial y} + z_i \frac{\partial h_i}{\partial z} + nh_i \quad (1)$$

where  $h_i = h(x_i, y_i, z_i)$  is the  $i$ th observation of the total-field anomaly at the coordinates  $(x_i, y_i, z_i)$ ,  $\eta$  is the structural index related to the nature or geometry of the source. The parameters to be estimated are  $\hat{x}_o, \hat{y}_o, \hat{z}_o$ , related to the horizontal and vertical coordinates of the source, and  $\hat{b}$ , a base level (i.e., a background value). By assuming a tentative structural index, Euler deconvolution is applied to the whole dataset using a moving data window scheme. At each window, we solve the linear system of  $N$  equations (equation 1) in four unknowns  $(\hat{x}_o, \hat{y}_o, \hat{z}_o, \hat{b})$ .

In the following tests, we generated three different magnetic sources that can be approximate by simple geometry (Hinze et al., 2013) with different structural indices (SI). We generated a line of poles simulating a vertical sheet (SI=1), a point pole simulating a vertical cylinder (SI=2) and a point dipole simulating a sphere (SI=3).

In our approach, we assign a tentative structural index to obtain estimates of the four parameters for each tentative structural index. We plotted all estimates using the procedure adopted by Silva and Barbosa (2003), the estimates are plotted against the  $x$ - and  $y$ -coordinates of the center of the moving data window used in Euler

deconvolution. These plots help us identify the estimates according to their patterns, so there is no need to reduce the number of solutions. Here, for the purpose of this study, we will only present plots of depth and base level estimates. Values of declination, inclination and total field intensity in synthetic tests were based on Chulliat et al. (2014). Here, derivatives are calculated in Fourier domain (Blakely, 1996)

### Constant base level

Figure 1 shows the synthetic noise-corrupted magnetic anomaly produced by three different sources, related to different structural indices. The anomaly is generated by a line of 1220 poles (SI=1) separated by grid distance, a monopole (SI=2) and a dipole (SI=3) of radius 0.5 km. The anomaly was corrupted with pseudorandom Gaussian noise with a standard deviation of 0.1 nT. The sources are magnetized by induction only, with a vertical direction. The line of poles extends from  $x_o = 15$  km to 258 km,  $y_o = 35$  km and  $z_o = 1.8$  km, each pole has magnetization intensity of 0.5 A/m. The single pole is located at  $x_o = 45$  km,  $y_o = 20$  km and  $z_o = 2$  km, with magnetization intensity of 4 A/m. Finally, the dipole is located at  $x_o = 25$  km,  $y_o = 20$  km and  $z_o = 1.5$  km, with magnetization intensity of 4 A/m. The survey was simulated on a grid of 325 points in x-coordinate (north direction) and 300 points in y-coordinate (east direction). Grid starts at  $x = y = 0$  and it is equally spaced at each 0.2 km, modeling was done at  $z = 0$  km, surface level. At the end of modeling, a constant base level of 65000 nT was added simulating the geomagnetic intensity at the magnetic pole. However, the results show in this test applies for a null base level, i.e., magnetic anomaly without IGRF.

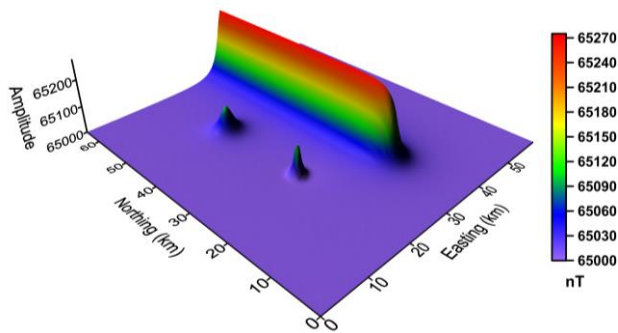


**Figure 1** – Magnetic anomaly with a base level equal to 65000 generated by 1) line of poles, 2) pole and 3) dipole vertically magnetized.

We apply Euler deconvolution using a  $9 \times 9$  moving data window and assuming structural indices 1, 2 and 3. Figure 2 (a) - (c) shows depth estimates from Euler deconvolution assuming indices 1, 2 and 3, respectively. For depth estimates, plateaus of solutions appear only when the correct SI is used. When the wrong structural index is used, depth estimates do not define a plateau; rather they form a cavity or a prominence. Thus, we can infer the correct structural index by the minimum variation

of those estimates. This procedure can be done comparing estimates using different structural indices for the same source.

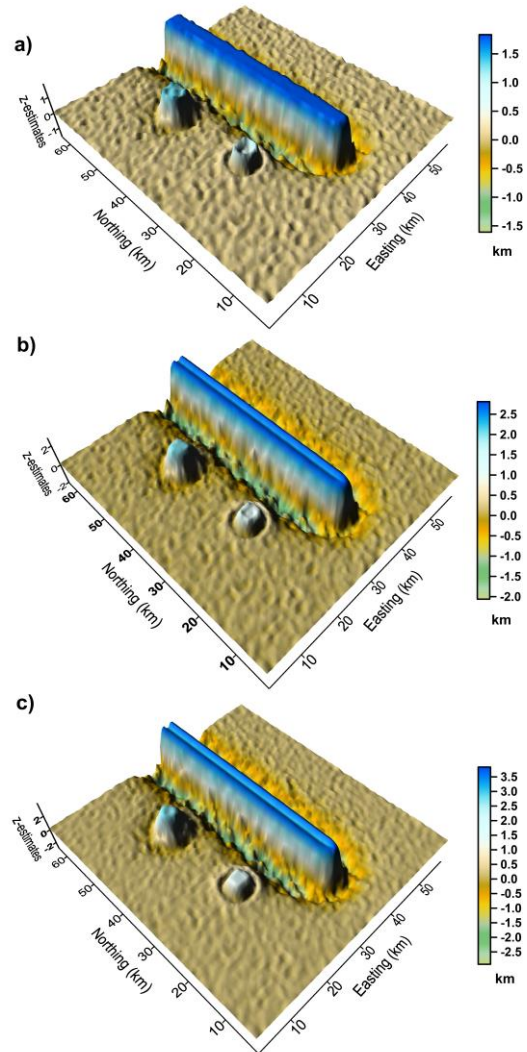


**Figure 2** – Depth estimates from Euler deconvolution using a  $9 \times 9$  moving data window assuming structural indices (a) 1, (b) 2 and (c) 3. Depth estimates using the correct structural index are constant over the source and have smallest variation.

Base level estimates from Euler deconvolution are in Figure 3 (a) – (c) assuming structural indices 1, 2 and 3, respectively. These estimates fall at the same positions as depth estimates and exhibit the same pattern when the correct structural index is used. Specifically a plateau of constant estimates is exhibited when the correct structural index is used. Comparing the same source at different base level estimates, we can easily see that the smallest variation of the estimates at source location indicates the correct structural index. Moreover, with this test we show that base level does not interfere at depth estimation, IGRF does not need to be previously removed to apply Euler deconvolution.

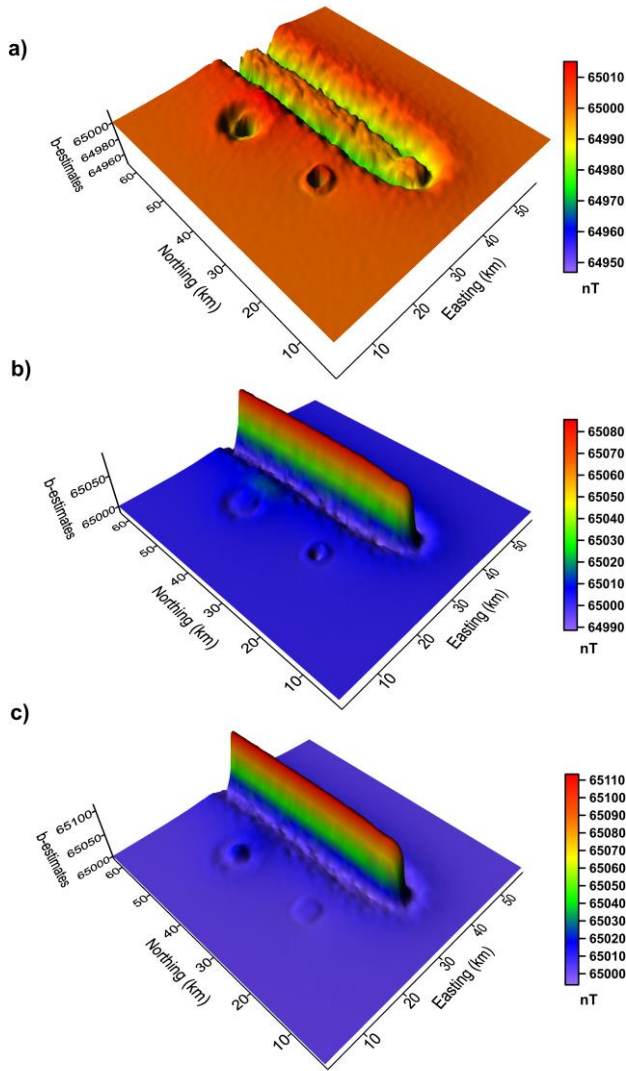


**Figure 3** – Base level-estimates of Euler deconvolution using a 9 x 9 moving data window assuming structural indices (a) 1, (b) 2 and (c) 3. Estimates using the correct structural index are constant over the source and have smallest variation.

**Nonlinear base level**

In this test, we generated a synthetic noise-corrupted magnetic anomaly produced by the three different sources of previous test and with the same magnetization. At the end of modeling we added a nonlinear base level, generated by:

$$H(x, y) = \frac{(x_i + 10) \times (y_i + 10)}{30}, \tag{2}$$

where the subscript *i* indicates grid location.

Figure 4a shows the nonlinear base level produced by equation 2 and Figure 4b the magnetic anomaly with the addition of the base level show in Figure 4a.

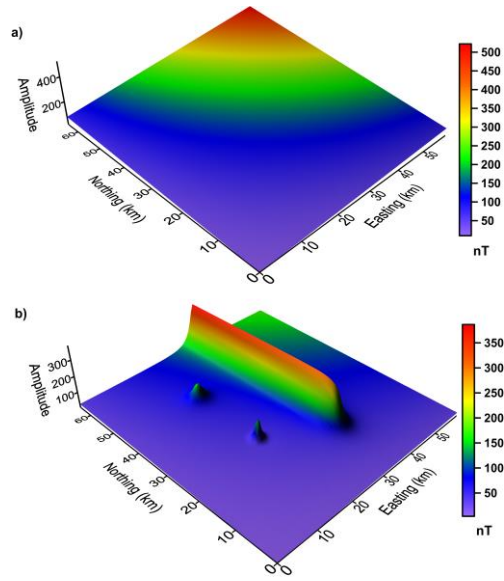


**Figure 4** – a) Nonlinear synthetic base level and b) Magnetic anomaly generated by a line of monopoles, a monopole and a dipole with the addition of the nonlinear base level shown in a).

We apply Euler deconvolution using a 9 x 9 moving data window, assuming structural indices 1, 2 and 3, and plotted depth and base level estimates. In Figure 5 (a) – (c) we can see depth estimates from Euler deconvolution assuming indices 1, 2 and 3, respectively. Figure 5 a) displays a plateau at the position of the line of poles, using SI = 1. This structural index SI = 1 is the correct one for the line of poles. However, in other plots is not easy to identify plateaus related to other indices. This is due to the nonlinear base level (or could be due to the proximity and interference of the sources). Although we can identify the location of the sources because of the plateaus, the minimum variation of depth estimates is no longer a valid option for cases like this, as shown in Table 1.

The first column of Table 1 shows the simulated source. The other columns show the values of the standard deviations for depth estimates using each tentative structural index. Minimum standard deviation for each source is in boldfaced. The minimum variation of estimates, i.e., the minimum standard deviation, for the pole indicates SI = 1, which is a wrong SI for this source. Let us recall that the correct structural index to a pole-like source is SI = 2. For the line of poles and dipole the minimum standard deviation of depth estimates indicate the correct source.

**Table 1** – Standard deviation of depth estimates. Minimum standard deviation for each source is in boldface.

Source	SI=1	SI=2	SI=3
Line of poles	<b>0.569820</b>	<b>0.075677</b>	0.117295
Pole	0.928046	0.091606	<b>0.066275</b>
Dipole	1.299238	0.133957	<b>0.030818</b>

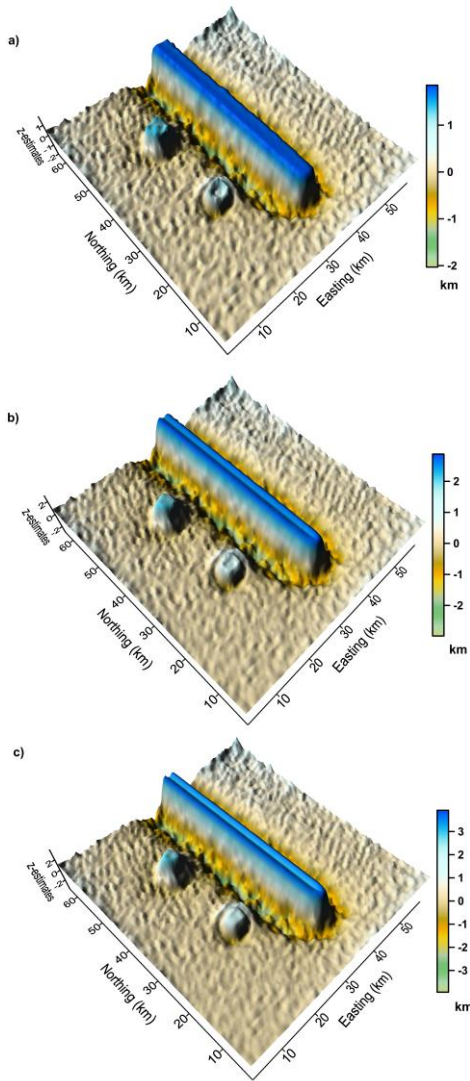


**Figure 5** – Depth estimates of Euler deconvolution using a 9 x 9 moving data window assuming structural indices (a) 1, (b) 2 and (c) 3. Plateaus, associated with correct SI, are not clearly identified, except for the case shown in a).

Figure 6 (a) - (c) shows base level-estimates from Euler deconvolution assuming structural indices 1, 2 and 3, respectively. Plateaus associated with minimum variation are much easier identified than via depth estimates. Notice that base level estimates are nonlinear for all cases; they increase toward north-east direction.

Table 2 shows the standard deviations of base level estimates which were calculated using the same area as in depth estimates (Table 1). In Table 2 is possible to see that the minimum variation of base level estimates (in boldface) confirms the correct structural index of each source. Therefore, base level estimates are more robust than depth estimates to define the correct structural index.

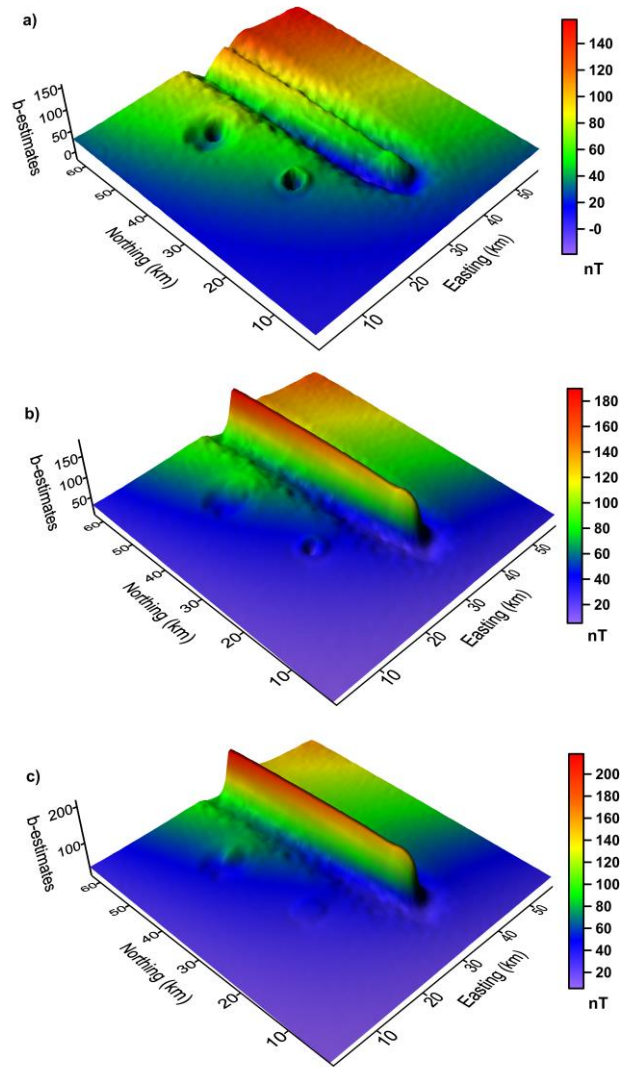


**Figure 6** – Base level-estimates of Euler deconvolution using a 9 x 9 moving data window assuming structural indices (a) 1, (b) 2 and (c) 3.

**Table 2** – Standard deviation of base level estimates. Minimum standard deviation for each source is in boldface.

Source	SI=1	SI=2	SI=3
<b>Line of poles</b>	<b>25.172398</b>	10.091611	19.717030
<b>Pole</b>	41.181648	<b>5.409108</b>	6.184976
<b>Dipole</b>	48.086922	6.145960	<b>2.990737</b>

**Real data application**

Figure 7 shows the magnetic anomaly over mafic-ultramafic alkaline bodies, in central Brazil (Dutra and Marangoni, 2009). This alkaline complex is surrounded by a Precambrian basement and the Phanerozoic sedimentary rocks of the Paraná basin (Dutra and Marangoni, 2009; Dutra et al., 2012; Marangoni and Mantovani, 2013). The flight height was approximately

constant about 100m from the terrain (approximately constant normal height of 500m). The magnetic anomaly in our study is known as Diorama.

In Figure 7 we can see that we have a strong anomaly, Diorama, but also many weak anomalies. As we will see later these sources producing weak anomalies may generate nonlinear base level (background).

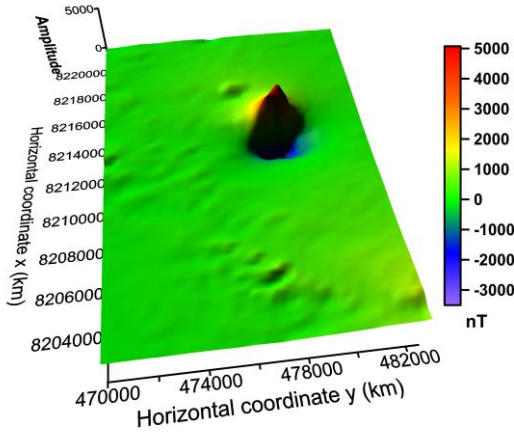


Figure 7 – Magnetic anomaly – Diorama.

We apply Euler deconvolution using a 35 × 35 moving data window, assuming structural indices 1, 2 and 3. In Figure 8 (a) – (c) we can see depth estimates and in Figure 8 (d) – (f) base level estimates in the right hand side, assuming indices 1, 2 and 3, respectively. From depth estimates, we can see many forms that seem plateaus. These plateaus can be related to the weak anomalies present in Figure 7. By inspecting depth estimates, shown in Figure 8 (a) – (c), is hard to see which structural index produced a plateau from Diorama. Base level estimates, Figure 8 (d) – (f), show a nonlinear pattern of all estimates from left to the right hand side. This nonlinear base level pattern may be generated by weak sources present in Figure 7 and some that are not in this Figure but in the vicinity. Notice that an initial analysis of base level estimates in Figure 8 (d) – (f) shows that the lowest range of estimates is associated to SI = 2 in Figure 8 (e). This analysis can be done comparing values of estimates at source position using the color bar. However, a quantitative analysis in the anomaly area is necessary to make sure it is the correct SI.

Table 3 shows the standard deviation of depth and base level estimates. The first column of Table 3 shows the kind of estimates, depth and base level. The other columns show the standard deviation for each structural index. Minimum standard deviation for each estimate is in boldface. The minimum variation of estimates, i.e., the minimum standard deviation, for depth estimates points to SI=1 and for base level estimates points to SI = 2. In the nonlinear base level test we observed a similar behavior. Depth estimates (Table 1) are more sensible to interfering anomalies than base level estimates (Table 2). Based on this analysis we may infer that Diorama may be generated by a source of SI = 2. The average of depth

estimates for SI = 2 gives the mean depth of the central part of the source as 671.30 m.

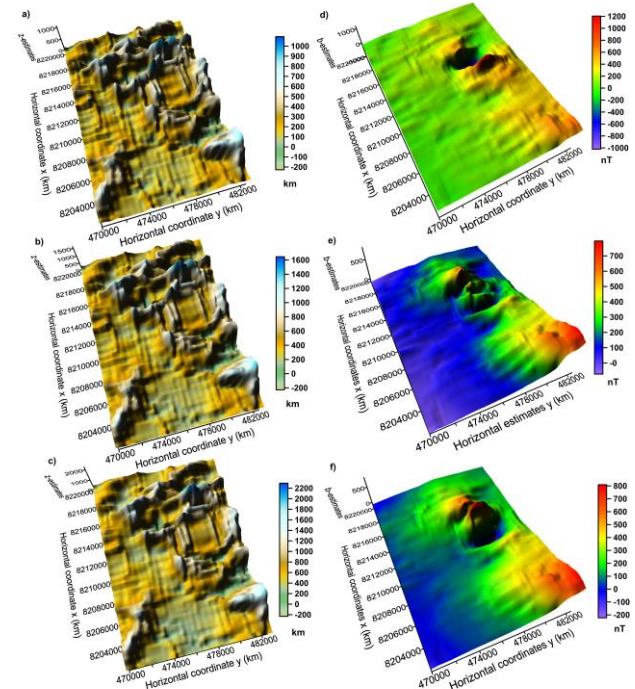


Figure 8 – Results of Euler deconvolution. Depth (a) – (c) and base level (d) – (f) estimates assuming SI: 1, 2 and 3, respectively for both estimates.

Table 3 – Standard deviation of depth and base level estimates for Diorama. Minimum standard deviation for each estimate is in boldface.

Estimate	SI=1	SI=2	SI=3
Depth	<b>137.960</b>	193.094	256.329
Base level	462.102	<b>60.281</b>	116.736

Conclusions

We presented a new approach to define the correct structural index with base level estimates. We calculated the standard deviation of base level estimates and showed that the minimum standard deviation indicates the correct structural index. In regions where interfering anomalies are present, base level estimates are nonlinear. In these cases, depth estimates are sensible to interfering anomalies and don't indicate the correct structural index. Plateaus associated with depth estimates give the location of the sources and minimum standard deviation of base level estimates at these positions gives the correct SI. When there are no interfering anomalies, plateaus, which indicates minimum variation of estimates at either depth or base level estimates, gives the correct SI. Our approach is simple and does not demand extra computational efforts than a simple math computation. We used constant and nonlinear base levels in our synthetic tests based on literature. Base level estimates for nonlinear case simulated what was observed in the same estimates for real data. Based on synthetic tests we

inferred the correct structural index for Diorama and thus the mean depth for the central part of the anomaly.

### Acknowledgments

F. Melo was supported in this research by a Phd scholarship from Coordenação de aperfeiçoamento de Pessoal de Nível Superior (CAPES), Brazil.

### References

- Barbosa, C.F., Silva, B.C., Medeiros, W.E., 1999. Stability analysis and improvement of structural index estimation in Euler deconvolution. *Geophysics* 64, 48–60. doi:10.1190/1.1444529
- Blakely, R.J., 1996. *Potential Theory in Gravity and Magnetic Applications*. Cambridge University Press.
- Chulliat, A., Macmillan, S., Alken, P., Beggan, C., Nair, M., Hamilton, B., Woods, A., Ridley, V., Maus, S., Thomson, A., 2014. The US/UK World Magnetic Model for 2015-2020. doi:10.7289/V5TH8JNW
- Dewangan, P., Ramprasad, T., Ramana, M. V., Desa, M., Shailaja, B., 2007. Automatic interpretation of magnetic data using euler deconvolution with nonlinear background. *Pure Appl. Geophys.* 164, 2359–2372. doi:10.1007/s00024-007-0264-x
- Dutra, A.C., Marangoni, Y.R., 2009. Gravity and magnetic 3D inversion of Morro do Engenho complex, Central Brazil. *J. South Am. Earth Sci.* 28, 193–203. doi:10.1016/j.jsames.2009.02.006
- Dutra, A.C., Marangoni, Y.R., Junqueira-Brod, T.C., 2012. Investigation of the Goiás Alkaline Province, Central Brazil: Application of gravity and magnetic methods. *J. South Am. Earth Sci.* 33, 43–55. doi:10.1016/j.jsames.2011.06.004
- Gerovska, D., Araúzo-Bravo, M.J., 2003. Automatic interpretation of magnetic data based on Euler deconvolution with unprescribed structural index. *Comput. Geosci.* 29, 949–960. doi:10.1016/S0098-3004(03)00101-8
- Hinze, W.J., von Frese, R.R.B., Saad, A.H., 2013. *Gravity and Magnetic Exploration*. Cambridge University Press, Cambridge. doi:10.1017/CBO9780511843129
- Hood, P., 1965. Gradient measurements in aeromagnetic surveying. *GEOPHYSICS* 30, 891–902. doi:10.1190/1.1439666
- Hsu, S., 2002. Imaging magnetic sources using Euler's equation. *Geophys. Prospect.* 50, 15–25. doi:10.1046/j.1365-2478.2001.00282.x
- Marangoni, Y.R., Mantovani, M.S.M., 2013. Geophysical signatures of the alkaline intrusions bordering the Paraná Basin. *J. South Am. Earth Sci.* 41, 83–98. doi:10.1016/j.jsames.2012.08.004
- Melo, F.F., Barbosa, V.C.F., Uieda, L., Oliveira Jr, V.C., Silva, J.B.C., 2013. Estimating the nature and the horizontal and vertical positions of 3D magnetic sources using Euler deconvolution. *Geophysics* 78, J87–J98. doi:10.1190/GEO2012-0515.1
- Ravat, D., 1996. Analysis of the Euler method and its applicability in environmental magnetic investigations. *J. Environ. Eng. Geophys.* 1, 229–238. doi:10.4133/JEEG1.3.229
- Reid, A.B., Allsop, J.M., Granser, H., Millett, A.J., Somerton, I.W., 1990. Magnetic interpretation in three dimensions using Euler deconvolution. *Geophysics* 55, 80–91. doi:10.1190/1.1442774
- Reid, A.B., Ebbing, J., Webb, S.J., 2014. Avoidable Euler Errors - the use and abuse of Euler deconvolution applied to potential fields. *Geophys. Prospect.* 62, 1162–1168. doi:10.1111/1365-2478.12119
- Reid, A.B., Thurston, J.B., 2014. The structural index in gravity and magnetic interpretation: Errors, uses, and abuses. *GEOPHYSICS* 79, J61–J66. doi:10.1190/geo2013-0235.1
- Silva, J.B.C., Barbosa, V.C.F., 2003. 3D Euler deconvolution: Theoretical basis for automatically selecting good solutions. *Geophysics* 68, 1962–1968. doi:10.1190/1.1635050
- Stavrev, P.Y., 1997. Euler deconvolution using differential similarity transformations of gravity or magnetic anomalies. *Geophys. Prospect.* 45, 207–246. doi:10.1046/j.1365-2478.1997.00331.x
- Thompson, D.T., 1982. EULDPH: A new technique for making computer-assisted depth estimates from magnetic data. *Geophysics* 47, 31. doi:10.1190/1.1441278